Source contributions to $PM_{2.5}$ under unfavorable weather systems in Guangzhou City, China

Wang Nan[1*], Ling Zhenhao[2], Deng Xuejiao[1], Deng Tao[1], Lyu Xiaopu[3], Li Tingyuan [4]

[1] Institute of Tropical and Marine Meteorology/Guangdong Provincial Key Laboratory of Regional Numerical Weather Prediction, CMA, Guangzhou, China

[2] School of Atmospheric Sciences, Sun Yat-sen University, Guangzhou, China

[3]Department of Civil and Environmental Engineering, The Hong Kong Polytechnic University, Hong Kong

[4] Ecological Meteorology Center, Guangdong Provincial Meteorological Bureau, Guangzhou, China.

Abstract

Historical haze episodes (2013 ~ 2016) in Guangzhou were examined and classified according to synoptic weather systems. Four types of weather systems were found to be unfavorable; among which foreside of a cold front (FC) and sea high pressure (SP) were the most frequent (> 75% of the total). Targeted case studies were conducted based on an FC-affected event and an SP-affected event with the aim of understanding the characteristics of the contributions of source regions to $PM_{2.5}$ in Guangzhou. Four kinds of contributions, namely, emissions outside Guangdong Province (super-region), emissions from the Pearl River Delta region (PRD region), emissions from Guangzhou-

[1] *Correspondence to: **N. Wang**, Institute of Tropical and Marine Meteorology/Guangdong Provincial Key Laboratory of Regional Numerical Weather Prediction, CMA, Guangzhou, China. Tel: +86 20 39456536, wangn@grmc.gov.cn

Foshan-Shenzhen (GFS region) and emissions from Guangzhou (local) were investigated using the Weather Research Forecasting – Community Multiscale Air Quality model. Our results showed that the source region contribution differed with different weather systems. SP was a stagnant weather condition, the source region contribution ratio showed that the local region was a major contributor (37%), while the PRD region, GFS region, and the super-region only contributed 8%, 2.8% and 7%, respectively, to $PM_{2.5}$ concentrations. By contrast, FC favored regional transport. The super-region became noticeable, contributing 34.8%, while the local region decreased to 12%. A simple method was proposed to quantify the relative impact of meteorology and emissions. Meteorology had a 35% impact compared with an impact of -18% for emissions when comparing the FC-affected event with that of the SP. The results from this study can provide guidance to policymakers for the implementation of effective control strategies.

Key words: Air pollution modeling, WRF-CMAQ, Guangzhou, Source contribution, Unfavorable weather system, $PM_{2.5}$

1. Introduction

Haze pollution, characterized by high levels of fine particles ($PM_{2.5}$, particles with a diameter less than 2.5 um) and low visibility, is of increasing concern in China. Ambient particles can affect air quality and climate because they can absorb and scatter solar irradiation (Qiu et al., 1985; Waston, 2002; Hyslop, 2009; Cao et al., 2012). They also pose an adverse effect on human health. Studies have shown that high concentrations of $PM_{2.5}$ can increase morbidity and mortality as well as affecting the cardiovascular system (Dockery et al., 1993; Tie et al., 2009; Pope et al., 2009; IPCC 2013).

Guangzhou is the capital of Guangdong Province and a mega city located in the city clusters of the Pearl River Delta (PRD) region. (The PRD often refers to nine cities in Guangdong Province, i.e., Guangzhou, Shenzhen, Dongguan, Foshan, Huizhou, Zhuhai, Zhongshan, Jiangmen, and Zhaoqing). With a population of more than 10 million, the city contributed $1.96x10^4$ hundred million yuan to the GDP, ranking first in Guangdong Province in 2016. (Guangdong Statistical Yearbook, 2016) However, the rapid urbanization and economic growth have resulted in this city suffering from severe air quality in the past. In fact, Guangzhou has often been under low-visibility conditions since the 1980s (Deng et al, 2008). During some extreme events, the daily average visibility can be less than 2 km with the AOD higher than 1.2 (Wu et al. 2005). High concentrations of $PM_{2.5}$ accompany these events (Tao et al. 2011; Zheng et al., 2011; Huang et al., 2013; Deng et al., 2014; Andersson et al., 2015; Mai et al., 2016). Facing enormous public pressure to ensure better air quality, the Chinese government has exerted considerable effort in mitigating air pollution in the past. Every Five-Year Plan

has set targets for primary emission control, and VOC emissions are going to be tightened in addition to controlling emissions of SO_2 and NO_x in the 13th Five-Year Plan (from 2016 to 2020). In 2013, the State Council released an "Air Pollution Action Plan", setting specific target for developed areas, among which a 15% reduction goal was set for PRD $PM_{2.5}$ concentrations. In the local region, a series of emission control strategies were implemented by the joint governments of Guangdong and Hong Kong. One example is the endorsed "PRD Air Pollutant Emission Reduction Plan Up to 2020". As a result, a declining trend of $PM_{2.5}$ in Guangzhou was measured between 2010 and 2015, with annual concentrations of 55, 41, 51, 53, 49 and 32 $\mu g/m^3$, respectively (Guangdong Year Book 2010-2015). Though the situation is becoming positive, there is still a long way to go as the annual $PM_{2.5}$ concentration significantly exceeds the WHO guideline (annual mean: 10 $\mu g/m^3$). For policymakers, understanding source contributions to ambient $PM_{2.5}$ concentration is the basis to further improve air quality in PRD.

In recent years, a series of studies were carried out to improve our knowledge of emissions and their contributions to ambient $PM_{2.5}$ in Guangzhou by using different methods, i.e., receptor models, tracing technology and chemical transport model (CTM) (Wang et al., 2004; Louie et al., 2005; Guo et al., 2009; Zhang et al., 2012; Gao et al., 2013). Xiao et al (2011) used observations and Positive Matrix Factorization (PMF) to identify sources of submicron organic aerosols in a rural site of Guangzhou, reporting that primary organic aerosol constituted ~34-47% of organic aerosol and secondary organic aerosol constituted ~53-66% of regional organic aerosol. Zheng et al (2011)

used Chemical Mass Balance (CMB) to conduct source apportionment of carbonaceous aerosols in Guangzhou. It was found that primary emissions were important sources of excess organic carbon in the PRD. In addition, tracing technology, such as the use of isotopes, is also a good method. Liu et al (2014) used radiocarbon (^{14}C) isotopes and tracers to conduct source apportionment of carbonaceous aerosols during winter in Guangzhou. Gao et al., (2012) combined PMF with tracer data and concluded that vehicular emissions, biomass burning and coal combustion were the main sources of polycyclic aromatic hydrocarbons in Guangzhou. Another mainstream method is the CTM. Wu et al (2013) adopted Comprehensive Air Quality Model together with Particulate Source Apportionment Technology (CAMx-PSAT) in Hong Kong/PRD and revealed that super-regional transport and mobile vehicles were the two major fine particle sources in most cities of PRD. Cui et al (2015) claimed that stationary sources (industrial and power) had largest contribution to $PM_{2.5}$ in Guangzhou after conducting simulations with Weather Research Forecasting coupled Chemistry (WRF-Chem). However, most previous studies were conducted to determine the possible contributions of individual sources, whereas few studies have focused on the impact of weather conditions since source contributions differ under different weather conditions. In fact, the lifetime of $PM_{2.5}$ components and their precursors are different: both the generated $PM_{2.5}$ components and their precursors can be transported from region to region depending on the synoptic weather system (Tan et al., 2009; Li et al., 2012; Liu et al., 2014). Furthermore, meteorological conditions also play important roles in the formation of secondary aerosols (Wang et al., 2009; Tan et al., 2013; Zhao et al., 2017).

Therefore, to control $PM_{2.5}$ pollution in a specific location, in addition to identifying the impact of local sources, the impact of regional/super-regional sources as well as meteorology must be identified, especially under unfavorable weather conditions. Understanding how much ambient $PM_{2.5}$ originates from different sources under unfavorable weather conditions is critical for improving air quality in the PRD region. In this study, source contribution studies are combined with synoptic meteorology. This combination can help to strengthen our knowledge of the characteristics of weather conditions during haze pollution, as well as help advance our knowledge of the contribution characteristics of a source region under a specific weather system. Since our present prediction ability and forecast period of weather systems are relatively better and longer than those of $PM_{2.5}$, the results from this study can provide guidance to policymakers so that targeted emission control can occur in advance.

Historical haze episodes (2013 ~ 2016) in Guangzhou were identified and classified according to weather systems. Case studies were performed by choosing two of the most unfavorable weather systems. We used a brute-force method with the aid of the WRF-CMAQ (Weather Research Forecasting - Community Multiscale Air Quality) model to obtain contributions of different sources to $PM_{2.5}$ in Guangzhou. Section 2 introduces the data used, the model system and the study method. Section 3 provides weather system analysis and observation analysis. Section 4 presents the evaluation of the modelling performance. The impact of source contributions and weather conditions are discussed in Section 5. Finally, section 6 summarizes the results.

2. Model, data and methodology

2.1 Model system

The U.S. Community Multi-scale Air Quality (CMAQ, version 4.7.1, http://cmascenter.org/cmaq/) model was used to simulate $PM_{2.5}$ concentrations under 2 different typical meteorological conditions. Developed by the U.S. Environmental Protection Agency (EPA), CMAQ is a 3-dimensional Eulerian chemical transport model. It is designed for applications such as atmospheric air quality research and policy analysis and regulation. The Weather Research and Forecasting (WRF, version 3.3.1, http://www.wrf-model.org/index.php) model was run to provide offline meteorological fields. The Meteorology Chemistry Interface Processor (MCIP, version 3.6) was used to convert the WRF-produced meteorological data to the format required by CMAQ. Previous studies have shown that the WRF-CMAQ system is a powerful tool in simulating air quality ranging from a city to a mesoscale level in China (Wang et al., 2010; Che et al., 2011; Wang et al., 2015).

The WRF-CMAQ configurations were generally consistent with a previous study (Wang et al., 2016). In brief, a two-way nested domain was adopted with a grid resolution of 27 km and 9 km, with horizontal grids of 283 × 184 and 223 × 163, respectively. The outer domain covered the whole continental region of China, and the inner domain covered the entire region of Guangdong Province with strong focus on the PRD region (see Fig. 1). The physical and chemical parameterization configurations were consistent with those presented in Wang et al. (2016).

We used the 2012-based Multi-resolution Emission Inventory for China (MEIC) to

147 provide anthropogenic emissions for all selected scenarios. MEIC is a series of emission
148 inventories for China and has a grid resolution of 0.25×0.25° (He 2012). It was
149 developed by Tsing Hua University and considered five emission categories, namely,
150 transportation, agriculture, power plants, industry and residence. In this study, MEIC
151 was linearly interpolated to the model domain with consideration of the earth's
152 curvature effect. For grids outside of China, the INDEX-B (Intercontinental Chemical
153 Transport Experiment-Phase B) Asian emission inventory (Zhang et al., 2009) was used.
154 The natural emissions for all scenarios were calculated offline using the Model of
155 Emissions of Gases and Aerosols from Nature (MEGAN, version 2.04, Guenther et al.,
156 2006).

157 **2.2 Unfavorable weather systems**

158 Studies have shown that air pollution in the PRD region is an integrated result of local
159 (sources in the city areas), regional (other city sources within the region) and super-
160 regional (all sources outside the study region) contributions (Kemball-Cook et al., 2009;
161 Li Ying et al, 2012). Understanding the specific contribution is fundamental for
162 designing effective emission control strategies. One challenge is that the source
163 contribution varies if weather conditions are different. In order to take weather impact
164 into account, historical haze episodes from 2013 to 2016 were identified and classified
165 according to weather systems. In this study, a haze episode was defined as a period with
166 at least 3 consecutive haze days (a haze day refers to daily visibility less than 10 km
167 and daily relative humidity less than 90%; rainy days are not considered). A similar
168 method can be found in Wu et al., (2007). These data were collected from 86 operational

automatic weather monitoring stations throughout Guangdong, and the data quality was well controlled by China Meteorology Administration (CMA). Weather systems were classified by artificially analyzing the concerning weather charts of the selected haze episode. Similar method can be found in previous study (Chan and Chan., 2000; Huang et al., 2006; Saskia et al., 2010; Li et al., 2011; Li et al., 2016;). According to this method, four types of weather systems, namely, foreside of a cold front (FC), sea high pressure (SP), equalizing pressure (EP) and others (Os, such as mainland high pressure and tropical cyclone) were diagnosed as unfavorable weather systems in Guangdong Province (see

Table 1). A general introduction of these weather systems is presented in the Supplementary material (Fig. S1) and more detailed information about the statistical data is given by Gao et al., (2018, under review). On the one hand, the 4-year statistical result showed that the haze episodes exhibited a declining trend. The total number of haze episodes from 2013 to 2016 was 61, 35, 30 and 19, respectively, which indicated that the emission control efforts were effective. The variation of annual concentrations of $PM_{2.5}$ also verified this positive aspect with $PM_{2.5}$ concentrations of 53, 49, 32 and 30μg/m^3, respectively. On the other hand, SP was the most frequent unfavorable weather system, accounting for 49.0% from 2013 to 2016. Among all the SP episodes, the lowest visibility (daily averaged) ranged from 0.7 km to 3.8 km with the highest concentrations of $PM_{2.5}$ (daily averaged) ranged from 80 μg/m^3 to 184 μg/m^3. FC was the second dominated unfavorable weather system, with the occurrence of 26.9%. Low visibility (0.6~5.4 km) and high $PM_{2.5}$ (79~222 μg/m^3) concentration was also recorded. EP and Os were the last two, with the occurrence of 16.6 and 7.6%, respectively. Since the total occurrence of haze episodes under SP and FC was over 75%, significantly higher than that under EP and Os ($p < 0.05$), targeted investigations were conducted by examining an SP-affected event (Nov. 19 ~ Nov. 25 2014) and an FC-affected event (Nov. 19 ~ Nov. 25 2010) with the aim of explaining the characteristics of source contributions under these 2 typical unfavorable weather systems.

2.3 Scenario Setting

Fig. 2 shows emissions categorized by administrative boundaries of provinces (Fig. 2a) and cities (Fig. 2b). It was shown that emissions (SO_2, NO_x, PMC, $PM_{2.5}$, CO and VOC)

200 from Guangdong were the highest among the 6 provinces in southern China, with a
201 total amount of 10.9 x 10^6 Mg/year (unit area: 60.7 Mg/year/km^2). Hunan ranked the
202 second (total area: 9.9 x 10^6 Mg/year; unit area: 46.7 Mg/year/km^2), followed by
203 comparative emissions from Guangxi (6.3 x 10^6 Mg/year; unit area: 26.6 Mg/year/km^2),
204 Jiangxi (total area: 5.9 x 10^6 Mg/year; unit area: 35.4 Mg/year/km^2) and Fujian (4.1 x
205 10^6 Mg/year; unit area: 33.1 Mg/year/km^2). For cities within Guangdong Province, the
206 inland 9 PRD cities accounted for almost 70% of the emissions of the whole province.
207 In particular, emissions from the GFS (Guangzhou, Foshan and Shenzhen) region were
208 high: emissions from Guangzhou were the highest (total area: 1.7 x 10^6 Mg/year; unit
209 area: 0.23 x 10^3 Mg/year/km^2), followed by Shenzhen (total area: 1.4 x 10^6 Mg/year,
210 the 2nd highest; unit area: 0.7 x 10^3 Mg/year/km^2) and Foshan (total area: 1.2 x 10^6
211 Mg/year, the 3rd highest; unit area: 0.31 x 10^3 Mg/year/km^2). In fact, these 3 cities were
212 topographically close to each other, the contribution of GFS emissions are of interest in
213 the following study.
214 Since the PRD is influenced by Asian monsoon circulations and the synoptic wind
215 becomes a northerly wind in autumn and winter, the above emission patterns suggest
216 that air quality in Guangzhou is likely to be influenced not only by local emissions but
217 also emissions from nearby cities or provinces. With the objective of studying source
218 contributions to Guangzhou, the term local referred to in this paper indicates emissions
219 from Guangzhou City, the term region refers to city sources within the PRD region, and
220 the term super-region implies contributions from sources (both anthropogenic and
221 biogenic) outside Guangdong Province. One baseline emission scenario (BASE) and 4

emission reduction scenarios (ONLY_GD, NO_PRD, NO_GFS and NO_GZ) were used to study the possible source contributions under two unfavorable weather conditions (Table 2).

BASE refers to the scenario where $PM_{2.5}$ concentrations are simulated with the participation of the entire county-level emission inventories; the result represents the overall $PM_{2.5}$ contribution from all local and regional/super-regional sources without any reductions. ONLY_GD excludes all emissions except those from Guangdong, while NO_PRD, NO_GFS and NO_GZ pertain to emission inventories without emissions from the respective PRD region, GFS region (Guangzhou, Foshan and Shenzhen), and GZ (Guangzhou City). By comparing the reduction scenarios with the baseline, contributions from different source regions could be identified. For example, the difference between ONLY_GD and BASE is the contribution from other provinces (super-regional contribution); similarly, the difference between NO_PRD and BASE, the difference between NO_GFS and BASE and the difference between NO_GZ and BASE are the contributions from the PRD region, the GFS region and the local region, respectively. Hence, the Difference (△) and Source Region Contribution Ratio (*SRCR*) are defined to quantify their specific contributions:

$$\triangle = \frac{\sum_{i=1}^{ngrid}(B_i - C_i)}{ngrid}$$

$$SRCR = \sum_{i=1}^{ngrid}\left(\frac{Bi - Ci}{Bi}\right) x\ 100\%$$

, where C is the $PM_{2.5}$ concentration simulated under an emission reduction scenario; B is the baseline $PM_{2.5}$ concentration; *ngrid* is the total grid number of Guangzhou coverage in the model domain; and B_i and C_i represent the $PM_{2.5}$ concentration within

Guangzhou simulated under the baseline and an emission reduction scenario, respectively. To sum up, △ (mass concentration variation) and *SRCR* (percentage variation) can reflect the impact of a source region on Guangzhou.

2.4 Data used and model evaluation

Hourly values of surface meteorological parameters such as temperature, wind, relative humidity and pressure were adopted from the China Meteorological Administration (CMA). Meteorological data were collected at 9 automatic weather stations in 9 cities in inland PRD and used either for case analysis or for model validation. The air quality monitoring data used in this study were obtained from the Guangdong Province Environmental Administration (GDEPA) and the Pearl River Delta Regional Air Quality Monitoring Network (PRDRAQM). The network consists of 16 sites with 13 sites in inner PRD and 3 sites in Hong Kong. Previous studies have shown that these sites are well maintained and performed well in both scientific research and operational service (Zhong et al., 2013; Wang et al., 2016). In order to understand the two episodes controlled by unfavorable weather systems in Guangzhou, analyses of observed data were conducted to obtain the specific characteristics.

Statistical metrics including the mean values (Obs_{mean} and Sim_{mean}), mean bias (MB, MB = Obs_{mean} - Sim_{mean}), normalized mean bias (NMB, $NMB = \sum_{i=1}^{n}[(Sim(i) - Obs(i))/\mathrm{Obs(i)}]$), root mean square error (RMSE, $RMSE = \sqrt{\frac{1}{n}\sum_{i=1}^{n}(Sim(i) - Obs(i))^2}$) and the index of agreement (IOA, $IOA = 1 - \frac{\sum_{i=1}^{n}(sim(i)-Obs(i))^2}{\sum_{i=1}^{n}(|Sim(i)-\overline{Obs}|+|Obs(i)-\overline{Obs}|)^2}$) were used to assess the simulated results. Usually, a modeling result is acceptable if the NMB and RMSE values are close to 0 and the IOA

266 value is close to 1 (Jiang et al. 2008, Wu et al., 2013; Wang et al. 2015, Wang et al.,
267 2016).

268 **3. Characteristics of observations**

269 **3.1 Analysis of weather systems**

270 Fig. 3 depicts the weather charts of a typical FC-affected event (20 LST on Nov 21,
271 2010) and a typical SP-affected event (08 LST on Nov 20, 2014). Usually, an FC-
272 affected weather system occurs in a relatively cold season such as autumn, winter or
273 early spring. On Nov 19, 2010, southern China experienced a mainland high (see Fig.
274 S2), while a low-pressure system occurred over the Tibetan Plateau on Nov 20, and this
275 low pressure developed in an easterly direction (see Fig. S2). Then, the Tibetan low
276 reached the mainland high on Nov 21 and finally formed a cold front to the northwest
277 of the PRD (Fig. 3a). Since the PRD was located on the foreside of this cold front, the
278 weather conditions in the PRD were directly influenced. Usually, the northern parts of
279 Guangdong experience a northerly cold wind, while the southern parts of Guangdong
280 experience a southerly warm and humid air flow from the South China Sea. A
281 convergence could elevate the warm humid air flow, forming an inversion layer over
282 the PRD region. Indeed, an inversion layer was observed during this FC-affected event
283 based on temperature sounding data at Qingyuan (in Guangzhou) and Kings Park (in
284 Hong Kong) (see Fig. S3 in Supplementary materials), confirming the accurate weather
285 system analysis. Under such a weather condition, air pollutants brought by the northerly
286 wind from upwind areas could easily be trapped and accumulate in the PRD, thus
287 causing air pollution.

An SP-affected weather system usually occurs in autumn, winter and spring. In most haze-related cases, the predecessor of a sea high is a mainland high (only a few are directly formed by a western Pacific subtropical high in summer). On Nov 19, 2014, a cold mainland high was moving easterly to the sea (Fig S4); this cold high transformed once it encountered the warm marine atmosphere, and finally a slightly weaker but much warmer sea high was formed on Nov 20 (Fig. 3b). With the high-pressure center located over the sea, the ridge of this high extended southwesterly to the PRD and became the dominant weather system in the PRD. The PRD surface was dominated by downward anticyclonic air flows resulting in static wind on the ground (this was confirmed by the observed surface wind, see Fig. 5). Hence, such a weather condition would be not conducive to atmospheric dispersion and diffusion.

3.2 Analysis of observations

Fig. 4 shows the patterns of wind, relative humidity, pressure, temperature, $PM_{2.5}$ concentration and visibility during the FC-affected event. During this event, relatively strong northerly winds (daily mean ws = 2 m/s) were observed before the haze day (Nov 21), indicating the possible transport of air pollutants from Guangzhou to its downwind areas. In addition, a noticeable decreasing trend of diurnal pressure was observed compared to the relatively stable diurnal variations of RH and temperature. This was consistent with the weather system analysis in Section 3.1 as the Tibet low that reached southern China was conducive to regional transport. After the convergence of the northerly prevailing wind caused by the cold front and the southerly prevailing wind from the South China Sea (see discussion in Section 3.1), haze days were observed

on Nov 21, Nov 22, and Nov 24 with the highest $PM_{2.5}$ concentrations of 110 ug/m^3, 102 ug/m^3, and 105 ug/m^3 and the lowest visibility of 0.9 km, 4 km and 2 km, respectively. Significant inverse relationships were observed between $PM_{2.5}$ concentration and visibility (r = -0.61) during these haze days. In addition, likely caused by the inversion layer, the wind pattern changed to weak southerly winds on the haze days (i.e., the daily mean wind speed on Nov 21 was only 1.0 m/s), suggesting the possible accumulation of air pollutants. Therefore, the relationship between the wind and $PM_{2.5}$ concentrations during this FC-affected event revealed that relatively strong northerly winds occurred before haze days (see Nov 19 and Nov 23 in Fig. 4), which may have played a role in transporting pollutants to Guangzhou, while the static southerly wind controlled the atmosphere on the haze days (see Nov 21, Nov 22 and Nov 24 in Fig. 4), which might play a role in decreasing pollutants in Guangzhou.

The SP-affected event showed a different pattern (Fig. 5): there were 3 consecutive haze days starting from Nov 20 through Nov 22, with the highest $PM_{2.5}$ concentration of 112 ug/m^3 and the lowest visibility of 0.9 km during the haze episode. Though the wind directions varied considerably, the wind speeds (WS) remained at rather low levels (mean WS = 0.9 m/s) during the haze event (Nov 20 ~ Nov 22). The low wind speed indicated a stagnant atmospheric situation since the PRD was fully controlled by SP. RH showed a stable variation with a mean value of 68.5%, indicating that the atmosphere was relatively dry. An increasing trend of temperature and a decreasing trend of pressure could be seen from Nov 19 to Nov 20. This could be explained by the weather system evolution. The mainland cold high transformed when it encountered

the warm marine atmosphere (see Section 3.1). Though the pressure in the PRD decreased, the magnitude of the pressure under this SP-affected event remained high; the mean value during this episode was 1018 hPa, noticeably higher than that of the FC-affected event (1011 hPa). Therefore, the characteristic weather conditions under an SP-affected haze episode include a relatively high temperature, low humidity, static winds and high pressure. The atmosphere was not conducive to air pollutant dispersion, and local emissions appeared to be the dominant sources.

4. Evaluation of model performance

Given the analyses of weather systems in Section 3.1 and the analyses of meteorological factors in Section 3.2, it was found that the characteristics of the SP-affected event and the FC-affected event chosen in this study were consistent with the general overview (given by Li et al., 2016) about feature analysis of the typical FC weather system and an SP weather system. Therefore, the two selected events could represent the general characteristics of SP and FC weather systems, respectively. Prior to using the modeling result to study the source contribution, an evaluation of model performance is necessary to verify the model simulation. The evaluation of the FC-affected event was presented previously (Wang et al., 2016), and the result showed that the simulation was well matched with the observation. Here, we present the evaluation of the SP-affected event. Table 3 shows the average statistical comparisons between the simulated and observed values in this region. In general, the MB and NMB of temperature (T), relative humidity (RH) and wind speed (WS) ranged between -1.9 ~ 1.2 and -0.01 ~ 1.3, respectively, showing the magnitudes matched well with the observations. The high values of IOA

for T (0.9) and RH (0.8) also indicated a good agreement between the observed and simulated values. It was noted that the simulated WS values were generally over-estimated; this could be due to the model resolution and the urban canopy structure. The grid resolution (9 km x 9 km) might be relatively coarse to reveal the real geography, and the PBL scheme does not consider the urban canopy structure; therefore, uncertainties exist in wind calculations as the distribution of urban morphology affects the surface-atmosphere energy budget (Jiang et al., 2008; Wang et al., 2015). Moreover, land surface modules, such as soil moisture, also result in uncertainty in the wind shear calculation (Li et al 2013 OSAT). Generally, the results were within the typical range of meteorological modeling studies (Chen et al., 2007; Wu et al., 2013; Cui et al., 2015; He et al., 2015; Wang et al., 2016).

The simulated $PM_{2.5}$ and O_3 concentrations were also evaluated. Three typical stations were selected as representatives (Huadu, a suburban site in northern Guangzhou, Panyu Middle School, an urban site in southern Guangzhou, and Xixiang, a coastal urban site in Shenzhen). Fig. 6 shows that the time series of simulated $PM_{2.5}$ and O_3 values matched well with the observations. The simulated average $PM_{2.5}$ was 55.2 ug/m^3, close to the observed value (53.1 ug/m^3). Surface O_3 was slightly over-estimated with an MB of -12.9 ppb. The trends of the simulation were also comparable with those observed (IOA values were 0.5 and 0.8 for $PM_{2.5}$ and O_3, respectively). In addition, an area comparison was conducted for $PM_{2.5}$ evaluation. Observed $PM_{2.5}$ concentrations collected from GDEPA monitoring sites were interpolated throughout Guangdong (see Fig. 7a; the figure was downloaded from the EMOS website:

http://10.12.12.211/emos/index) and used to compare with simulations. It could be seen that high $PM_{2.5}$ concentrations were located in central Guangdong, i.e., the area where Guangzhou and Foshan are located; the concentrations were relatively well reproduced by the model. Overall, the spatial distributions showed that modelled $PM_{2.5}$ values agreed well with observations, indicating that the model also captured the regional pollution characteristics.

5. Source contributions

5.1 Impact of local, regional, and super-regional emissions

The spatial impact of emissions from different source regions during the SP-affected event is shown in Fig. 8. Under such a stagnant weather condition, emissions outside Guangdong had limited influence on most cities throughout Guangdong. It could be seen that the main affected areas were those provincial boundaries where $PM_{2.5}$ concentrations decreased by 15 ~ 18 $\mu g/m^3$. However, a rather limited influence was observed in most PRD cities, for example, the $PM_{2.5}$ concentration in Guangzhou only decreased by 0 ~ 3 $\mu g/m^3$. Indeed, the average $\triangle$ (difference) between ONLY_GD and BASE was 2.3 $\mu g/m^3$ in Guangzhou (Table 4). Compared to the influence of emissions outside Guangdong, emissions from the PRD region, GFS region and Guangzhou City mainly affected the $PM_{2.5}$ concentrations in areas within their specific administrative boundaries (Fig. 8 b-d). Noticeable reductions in $PM_{2.5}$ were measured in Guangzhou; the $\triangle$ was 19.6 $\mu g/m^3$, 16.4 $\mu g/m^3$ and 14.3 $\mu g/m^3$ without the consideration of PRD regional emissions, GFS regional emissions and Guangzhou local emissions, respectively (Table 4). However, little influence could be found in areas

outside these source regions. Such results suggested that the atmosphere was not favorable for regional transport, and local emissions became the dominant sources under the SP-affected weather conditions.

The spatial impact of super-regional, regional and local emissions indicated different patterns under the FC-affected event. Emissions from outside Guangdong played a dominant role in contributing $PM_{2.5}$ to most areas of Guangdong. The area mean $PM_{2.5}$ concentrations were reduced by 15.5 ug/m^3 if these emissions were not considered. In fact, the average △ between ONLY_GD and BASE was 14.3 ug/m^3 (Table 4), significantly higher than that of the SP-affected event ($p < 0.05$), indicating that super-regional transport became an important contributor under the FC-affected weather system. With respect to the impact of regional emissions (NO_PRD – BASE and NO_GFS - BASE) and local emissions (NO_GZ - BASE), the spatial differences in $PM_{2.5}$ concentrations displayed a "tongue-like" shape extending from the source regions to the southwest. The average △ of the PRD region, the GFS region and Guangzhou local was 10.3 μg/m^3, 8.7 μg/m^3 and 7.6 μg/m^3, with maximal reductions of 37 μg/m^3, 27.3 μg/m^3 and 22.2 μg/m^3, respectively (see Table 4). It should be noted that these three source region's contributions decreased while the contributions from emissions outside Guangdong increased compared to those under the SP-affected event. Such phenomena were consistent with the weather system analysis, i.e., the cold front resulted in a northerly wind in the PRD that transported air pollutants from source regions to downwind areas, thus resulting in the "tongue-like" shape. This finding also explained why super-regional transport became dominant under this condition, while

420 the SP-affected event was a more stable condition since downward air flow dominated
421 the atmosphere, trapping and accumulating emissions from source regions.
422 The contributions of specific source regions to $PM_{2.5}$ under these two typical
423 unfavorable weather systems are presented in Fig 10. When the sea high pressure
424 system controlled weather conditions in the PRD, the SRCR of the PRD region ($SRCR_{PRD\ region}$), the SRCR of the GFS region ($SRCR_{GFS\ region}$) and the SRCR of Guangzhou
426 ($SRCR_{Guangzhou}$) were 44.0%, 38.8% and 36.0%, respectively, which were all
427 significantly higher than that of the super-region ($SRCR_{super\text{-}region}$, 7.0%). It should be
428 noted that both the $SRCR_{PRD\ region}$ and the $SRCR_{GFS\ region}$ contained the source region
429 contributions from Guangzhou; we used the difference between the regional values and
430 the local values to deduct the contributions from Guangzhou. For example, the
431 difference between $SRCR_{PRD\ region}$ and $SRCR_{Guangzhou}$ is the source contribution from
432 the 8 other inland PRD cities (excluding Guangzhou). It was found that the 8 other
433 inland PRD cities contributed 8%, whereas Foshan and Shenzhen contributed 2.8%.
434 The results implied that local emissions were the major contributors to haze pollution,
435 and it is strongly suggested that local emissions be reduced when formulating emission
436 control strategies under a high-pressure system. With regard to the FC-affected event,
437 the super-regional source became the dominant contributor (Fig 10b) in Guangzhou.
438 The $SRCR_{super\text{-}region}$ was 34.8%, significantly higher than that of the SP-affected event
439 (SRCR = 7%, $p < 0.05$). In addition, the “tongue-like” shape in Fig. 9 indicated that
440 regional transport should be noticeable, and the calculation of SRCR showed that
441 regional source contributions were rather close to that of the local region ($SRCR_{PRD}$

$_{region}$, SRCR $_{GFS\ region}$ and SRCR $_{Guangzhou}$ were 16.0%, 13.6% and 12.0%, respectively). This is because Guangzhou is upwind in the PRD region, and the regional impact had greater influence in the downwind areas than in Guangzhou. Consequently, the super-regional contributions (emissions from the upwind area of Guangzhou) became dominant. Our results suggest that merely controlling local emissions under this weather condition is somewhat ineffective. By contrast, regional joint prevention and control should be considered to ensure a more reasonable control of haze pollution.

5.2 Impact of weather conditions.

The above analysis demonstrates that source contributions to $PM_{2.5}$ in Guangzhou exhibit different characteristics under different weather systems. In fact, haze pollution is the integrated result of unfavorable weather conditions and emissions. In this section, we propose a simple method to distinguish the relative impact of meteorology and emissions.

Fig. 11 presents the flowchart of this method. The observed difference (OBS_{diff}) can be directly calculated by comparing the observed $PM_{2.5}$ concentration of the SP-affected event and the FC-affected event. This OBS_{diff} can be regarded as the result of the difference between meteorology ($METE_{diff}$) and that of emissions ($EMIS_{diff}$) during two different periods. Then, $METE_{diff}$ can be obtained with the aid of CTM. By using the same emissions ($EMIS_{2012\text{-}MEIC}$, the November emission inventory from the 2012-MEIC) and different meteorologies ($METE_{FC\text{-}affected}$ and $METE_{SP\text{-}affected}$, produced by the WRF model) as input to drive the CMAQ model, the difference of the two simulations is $METE_{diff}$. Finally, $EMIS_{diff}$ can also be quantified after calculating

464 OBS_{diff} and $METE_{diff}$. We know this method has uncertainties; the main uncertainty is
465 introduced through the accuracy of model performance. For example, the emission
466 inventory contains uncertainties itself, parameter schemes in numerical models can also
467 bring uncertainties, and the over-estimated surface wind may decrease air pollutants in
468 upwind areas and increase simulation results in downwind areas. However, since the
469 simulated results have already passed a strict evaluation, the results are considered
470 acceptable. Furthermore, through the rapid development of numerical models, the
471 uncertainy associated with the model has shown a decreasing trend. Therefore, this
472 simple algorithm can be regarded as a means to quantify the relative impact of
473 emissions and meteorology.
474 Fig. 12 presents the relative impact of meteorology and emissions in two events, i.e.,
475 35% and -18%, respectively. This result is consistent with the above analysis. On the
476 one hand, the SP-affected event was a stagnant condition, and local emissions were the
477 major contributors. On the other hand, super-regional transport was more important
478 than local emissions for the FC-affected event. Therefore, the relative impact of
479 meteorology was positive while the impact of emissions was negative when comparing
480 the FC and SP-affected events.

481 **6. Summary**

482 In this study, source contribution studies were combined with synoptic meteorology to
483 understand the contribution characteristics of source regions under different
484 unfavorable weather systems.
485 Historical haze episodes (2013 ~ 2016) in Guangzhou were examined and classified

according to synoptic weather systems. Four types of weather systems were diagnosed as unfavorable: SP was ranked first (49.0%), followed by FC (26.9%), EP (16.6%) and Os (7.6%), respectively, in terms of the total number of haze events. Since the occurrence of FC and SP were the highest (> 75% of the total haze episodes), targeted case studies were performed of an SP-affected event and an FC-affected event. Monitoring data showed that SP was characterized by low winds (0.9 m/s), relatively high pressure (1018 hPa) and low relative humidity (68.5%). The high pressure-controlled system resulted in a rather stable atmosphere, thus pollutants were trapped and were not easily diffused. By contrast, FC was more favorable for pollutant transport. The cold front moved in a southeasterly direction, and synoptic winds prevailed in Guangdong. Northerly winds dominated and persisted at relatively high levels (2 m/s). Such a wind pattern was conducive to the transport of pollutants from upwind to downwind areas.

The numerical source regions' contribution results were consistent with the meteorological analysis. The source regions' contributions depicted different characteristics when different weather systems dominated. SP was a stagnant weather condition; the SRCR showed that the local region was a major contributor (37%) while the contributions of the PRD region (excluding Guangzhou), GFS region (excluding Guangzhou) and super-region were only 8%, 2.8% and 7%, respectively. By contrast, FC favored regional transport. The super-region became noticeable, contributing 34.8%, while the local region decreased to 12%. A simple method was proposed to quantify the relative impact of meteorology and emissions. The meteorological impact was 35%

while that of emissions was -18% when comparing the FC-affected event with the SP-affected event.

Our results highlight the importance of the meteorological impact on the source region contribution. Attention should be paid to local emissions when an SP-type system dominates, while regional joint control should be initiated when an FC-type system is in control. This study can provide guidance to policymakers to implement effective control strategies under unfavorable weather systems.

Acknowledgement

This study was supported by the National Natural Science Foundation of China (41475105), National Key Project of MOST (2016YFC0202003), Guangdong province science and technology plan (Grant No. 2015A020215020), national science and technology support program (2014BAC16B00), the science and technology innovative research team plan of Guangdong Meteorological Bureau (201506), the science and technology study project of Guangdong Meteorological Bureau (2015Q03) and Guangdong province Science and Technology Plan (2015A020215020 and 2013B030200001). The author also thanks Tsinghua University for providing MEIC.

Reference

Andersson, A. *Deng J.J., Du K, et al.*, 2015: Regionally-varying combustion sources of the January 2013 severe haze events over eastern China, *Environmental science & technology* **49**, pp. 2038-2043.

Cao, J.J, Wang Q. Y., *Chow J. C., et al.*, 2012: Impacts of aerosol compositions on visibility impairment in Xi'an, China, *Atmospheric Environment* **59**, pp. 559-

566.

Che, W., Zheng, J., Wang, S., Zhong, L., Lau, A., 2011: Assessment of motor vehicle emission control policies using Model-3/CMAQ model for the Pearl River Delta region, China, *Atmospheric Environment* **45**, pp. 1740-1751.

Chen, D.S., Cheng, S.Y., Liu, L., Chen, T., Guo, X.R., 2007: An integrated MM5–CMAQ modeling approach for assessing trans-boundary PM10 contribution to the host city of 2008 Olympic summer games—Beijing, China, *Atmospheric Environment* **41**, pp. 1237-1250.

Cui, H., Chen W.H., Dai W., *et al.*, 2015: Source apportionment of PM2.5 in Guangzhou combining observation data analysis and chemical transport model simulation, *Atmospheric Environment* **116**, pp. 262-271.

Deng, T. *Wu D., Deng XJ., et al.*, 2014: A vertical sounding of severe haze process in Guangzhou area, *Science China Earth Sciences* **57**(2014), pp. 2650-2656.

Dockery, D.W., Pope, C.A., Xu, X., Spengler, J.D., Ware, J.H., Fay, M.E., Ferris, B.G., Speizer, F.E., 1993. An association between air pollution and mortality in six US cities. N. Engl. J. Med. 329 (24), 1753–1759.

Gao, B. *Guo H, Wang X.M., et al.*, 2013: Tracer-based source apportionment of polycyclic aromatic hydrocarbons in PM2.5 in Guangzhou, southern China, using positive matrix factorization (PMF), *Environmental science and pollution research international* **20**, pp. 2398-2409.

Guo, H. *Ding A.J., So K.L.,et al.*, 2009: Receptor modeling of source apportionment of Hong Kong aerosols and the implication of urban and regional contribution,

Atmospheric Environment **43**(2009), pp. 1159-1169.

Guenther, A., Karl, T., Harley, P., Wiedinmyer, C., Palmer, P.I., Geron, C., 2006.Estimates of global terrestrial isoprene emissions using MEGAN (model of emissions of gases and aerosols from nature). Atmos. Chem. Phys. 6, 3181–3210.

He, H. *Tie X.X., Zhang Q., et al.*, 2015: Analysis of the causes of heavy aerosol pollution in Beijing, China: A case study with the WRF-Chem model, *Particuology* **20**, pp. 32-40.

He, K.B., 2012.Multi-resolution emission inventory for China (MEIC): model framework and 1990–30 2010 anthropogenic emissions. International Global Atmospheric Chemistry Conference

Huang, R.J. *Zhang Y.L., Bozzetti C., et al.*, 2014: High secondary aerosol contribution to particulate pollution during haze events in China, *Nature* **514**, pp. 218-222.

Hyslop, N.P., 2009: Impaired visibility: the air pollution people see, *Atmospheric Environment* **43**, pp. 182-195.

IPCC, 2013. Climate Change 2013: the Physical Science Basis. Working Group 1Contribution to the Fifth Assessment Report of the International Panel onClimate Change.

Jahn, H.J. *Kraemer A., Chen X.C., et al.*, 2013: Ambient and personal PM2.5 exposure assessment in the Chinese megacity of Guangzhou, *Atmospheric Environment* **74**, pp. 402-411.

Jiang, F., Wang, T., Wang, T., Xie, M., Zhao, H., 2008: Numerical modeling of a

574 continuous photochemical pollution episode in Hong Kong using WRF–chem,
575 *Atmospheric Environment* **42**, pp. 8717-8727.
576 Kemball-Cook, S. *Parrish D., Ryerson T., et al.*, 2009: Contributions of regional
577 transport and local sources to ozone exceedances in Houston and Dallas:
578 Comparison of results from a photochemical grid model to aircraft and surface
579 measurements, *Journal of Geophysical Research* **114**.
580 Kim, B.-U., Bae, C., Kim, H.C., Kim, E., Kim, S., 2017: Spatially and chemically
581 resolved source apportionment analysis: Case study of high particulate matter
582 event, *Atmospheric Environment* **162**, pp. 55-70.
583 Louie, P.K., Chow J.C., Chen A L.-W., *et al.*, 2005: PM2.5 chemical composition in
584 Hong Kong: urban and regional variations, *The Science of the total environment*
585 **338**, pp. 267-281.
586 Li, Y., Lau, A.K.H., Fung, J.C.H., Ma, H., Tse, Y., 2013: Systematic evaluation of ozone
587 control policies using an Ozone Source Apportionment method, *Atmospheric*
588 *Environment* **76**, pp. 136-146.
589 Li, Y., Lau, A.K.H., Fung, J.C.H. *et al.*, 2012: Ozone source apportionment (OSAT) to
590 differentiate local regional and super-regional source contributions in the Pearl
591 River Delta region, China, *Journal of Geophysical Research: Atmospheres* **117**,
592 pp. n/a-n/a.
593 Liu, J. *Li J, Zhang Y., et al.*, 2014: Source apportionment using radiocarbon and organic
594 tracers for PM2.5 carbonaceous aerosols in Guangzhou, South China:
595 contrasting local- and regional-scale haze events, *Environmental science &*

technology **48**, pp. 12002-12011.

Mai, J., Deng T., Yu L., *et al.*, 2016: A Modeling Study of Impact of Emission Control Strategies on PM2.5Reductions in Zhongshan, China, Using WRF-CMAQ, *Advances in Meteorology* **2016**, pp. 1-11.

Pope, C.A., Ezzati, M., Dockery, D.W., 2009.Fine particulate air pollution and life expectancy in the United States. New Engl. J. Med. 360 (4), 376–386.

Qiu, J.inhuan, Wang Hongqi, Zhou Xiuji, LuDaren., 1985: Experimental study of remote sensing of atmospheric aerosol size distribution by combined solar extinction and forward scattering method, Advances in Atmospheric Science, volume2, issue 3, pp 307-315

Streets, D.G., Fu J., Jang C.J., *et al.*, 2007: Air quality during the 2008 Beijing Olympic Games, *Atmospheric Environment* **41**, pp. 480-492.

Tan, J., Duan J., He KB, *et al.*, 2009: Chemical characteristics of PM2.5 during a typical haze episode in Guangzhou, *Journal of Environmental Sciences* **21**, pp. 774-781.

Tan, J. *Guo S., Ma Y., et al.*, 2011: Characteristics of particulate PAHs during a typical haze episode in Guangzhou, China, *Atmospheric Research* **102**, pp. 91-98.

Tan H.B., Yin Y., Gu X.S., Li F., Chan P.W., Xu H.B., Deng X.J., Wan Q.L., 2013: An observational study of the hygroscopic properties of aerosols over the Pearl River Delta region, Atmospheric Environment 77, 817-826

Tao, J. *Cao JJ., Zhang RJ., et al.*, 2012: Reconstructed light extinction coefficients using chemical compositions of PM2.5 in winter in Urban Guangzhou, China,

618 *Advances in Atmospheric Sciences* **29**, pp. 359-368.
619 Tie, X., Wu, D., Brasseur, G., 2009: Lung cancer mortality and exposure to atmospheric
620 aerosol particles in Guangzhou, China, *Atmospheric Environment* **43**, pp. 2375-
621 2377.
622 Wang, N., Guo, H., Jiang, F., Ling, Z.H., Wang, T., 2015: Simulation of ozone formation
623 at different elevations in mountainous area of Hong Kong using WRF-CMAQ
624 model, *The Science of the total environment* **505**, pp. 939-951.
625 Wang, N. *Lyu XP., Deng XJ., et al.*, 2016: Assessment of regional air quality resulting
626 from emission control in the Pearl River Delta region, southern China, *The*
627 *Science of the total environment* **573**, pp. 1554-1565.
628 Wang, X., Bi, X., Sheng, G., Fu, J., 2006: Chemical composition and sources of PM10
629 and PM2.5 aerosols in Guangzhou, China, *Environmental monitoring and*
630 *assessment* **119**, pp. 425-439.
631 Wang, X et al., 2009: Impacts of weather conditions modified by urban expansion on
632 surface ozone: Comparison between the Pearl River Delta and Yangtze River
633 Delta regions, Advances in Atmospheric Sciences, Volume 26, Issue 5, pp 962-
634 972
635 Wang, X. *Zhang Y., Hu Y., et al.*, 2010:Process analysis and sensitivity study of regional
636 ozone formation over the Pearl River Delta, China, during the PRIDE-PRD2004
637 campaign using the Community Multiscale Air Quality modeling system,
638 *Atmospheric Chemistry and Physics* **10**, pp. 4423-4437.
639 Watson, J.G., 2002: Visibility: Science and Regulation, *Journal of the Air & Waste*

Management Association **52**, pp. 628-713.

Wang, X., Carmichael, G., Chen, D., Tang, Y., Wang, T., 2005: Impacts of different emission sources on air quality during March 2001 in the Pearl River Delta (PRD) region, *Atmospheric Environment* **39**, pp. 5227-5241.

Wu, D., Fung, J.C.H., Yao, T., Lau, A.K.H., 2013: A study of control policy in the Pearl River Delta region by using the particulate matter source apportionment method, *Atmospheric Environment* **76**, pp. 147-161.

Wu D., Deng XJ., Bi XY., Li F., Tan HB., Liao GL., 2007; Study on the visibility reduction caused by atmospheric haze in Guangzhou area. Journal of Tropical Meteorology, 1006-8775, 02-0077-04

Wu, D., Tie XX., Li CC., *et al.*, 2005: An extremely low visibility event over the Guangzhou region: A case study, *Atmospheric Environment* **39**(2005), pp. 6568-6577.

Xiao, R., Takegawa N., Zheng M., *et al.*, 2011: Characterization and source apportionment of submicron aerosol with aerosol mass spectrometer during the PRIDE-PRD 2006 campaign, *Atmospheric Chemistry and Physics* **11**, pp. 6911-6929.

Xing, J. *Zhang Y., Wang SX., et al.*, 2011: Modeling study on the air quality impacts from emission reductions and atypical meteorological conditions during the 2008 Beijing Olympics, *Atmospheric Environment* **45**, pp. 1786-1798.

Zhao, B., Liou KN., Gu Y., *et al.*, 2017: Enhanced $PM_{2.5}$ pollution in China due to aerosol-cloud interactions, *Scientific reports* **7**, p. 4453.

662 Zhang, Q., Streets, D. G., Carmichael, G. R., He, K. B., Huo, H., Kannari, A., Klimont,
663 Z., Park, I. S., Reddy, S., Fu, J. S., Chen, D., Duan, L., Lei, Y., Wang, L. T., and
664 Yao, Z. L. (2009), Asian emissions in 2006 for the NASA INTEX-B mission,
665 Atmos. Chem. Phys., 9, 5131-5153.
666 Zhang, H. *Li JY., Ying Q., et al.*, 2012: Source apportionment of PM2.5 nitrate and
667 sulfate in China using a source-oriented chemical transport model, *Atmospheric*
668 *Environment* **62**, pp. 228-242.
669 Zheng, M. *Wang F., Hagler G.S.W., et al.*, 2011: Sources of excess urban carbonaceous
670 aerosol in the Pearl River Delta Region, China, *Atmospheric Environment* **45**,
671 pp. 1175-1182.
672 Zhong, L., Louie, P.K.K., Zheng, J., et al., 2013.The Pearl River Delta regional air
673 quality monitoring network–regional collaborative efforts on joint air quality
674 management. Aerosol Air Qual. Res.
675
676
677
678
679
680
681
682

683 Table 1 Occurrence and percentage of haze episodes classified according to weather

684 systems in Guangdong from 2013 to 2016

	Total number of haze episodes		FC [a]		SP [b]		EP [c]		Os [d]	
	No.[e]	% [f]	No.	%	No.	%	No.	%	No.	%
2013	61	\	20	32.8%	28	45.9%	9	14.8%	4	6.6%
2014	35	\	11	31.4%	14	40.0%	7	20.0%	3	8.6%
2015	30	\	6	16.7%	19	60.0%	4	13.3%	3	10.0%
2016	19	\	3	15.8%	11	57.9%	4	21.1%	1	5.3%
all	145	\	39	26.9%	71	49.0%	24	16.6%	11	7.6%

685 [a] FC: foreside of a cold front.

686 [b] SP: sea high pressure

687 [c] EP: equalizing pressure

688 [d] Os: other types of weather systems

689 [e] No.: number of haze episodes during the year

690 [f] %: percentage of haze episodes during the year

691

692 Table 2 Emission scenario setting for an FC-affected event and an SP-affected event

Weather System	Case label	Emission description	Purpose
S1: An FC-affected event (Nov. 19 ~ Nov. 25 2010) S2: An SP-affected event (Nov. 19 ~ Nov. 25 2014)	BASE	Normal Emission	To compare with the other scenario.
	ONLY_GD	Emissions only from Guangdong.	To investigate the contribution from other provinces (super-regional contribution)
	NO_PRD	Emissions except those from the PRD region	To investigate the contribution from the PRD region (PRD regional contribution)
	NO_GFS	Emissions except those from three major cities (Guangzhou, Foshan and Shenzhen, GFS)	To investigate the contribution from the GFS region (GFS regional contribution)
	NO_GZ	Emissions except those from Guangzhou	To investigate the contribution from Guangzhou city (local contribution)

693
694

Table 3 Averaged model performance of temperature, relative humidity, wind, $PM_{2.5}$ and O_3 during the SP-affected event (Nov 20 ~ Nov 25, 2014)

Simulated variables	Mean		MB	NMB	RMSE	IOA
	Obs	Sim				
T (°C)	22.5	21.3	1.2	-0.01	2.1	0.9
RH (%)	77.4	69.2	8.2	-0.1	10.7	0.8
WS (m/s)	1.6	3.5	-1.9	1.3	2.2	0.4
$PM_{2.5}$ (ug/m3)	53.1	55.2	-2.1	0.2	29.6	0.5
O_3 (ppb)	31.4	44.3	-12.9	0.5	28.3	0.8

699 Table 4 Statistics of $PM_{2.5}$ concentrations from different source regions during haze

700 days in Guangzhou

Parameter		Super-region		PRD region		GFS region		The local	
		SP	**FC**	**SP**	**FC**	**SP**	**FC**	**SP**	**FC**
△	Max	0.1	0	1.8	0.2	1.5	0.2	1.4	0.2
(μg/	Min	4.7	56.1	38.6	37.0	32.2	27.3	30.2	22.2
m^3)	Ave	2.3	14.3	19.6	10.3	16.4	8.7	14.3	7.6
SRCR		7.0%	34.8%	44.0%	16.0%	38.8%	13.6%	37.0%	12%

701

702

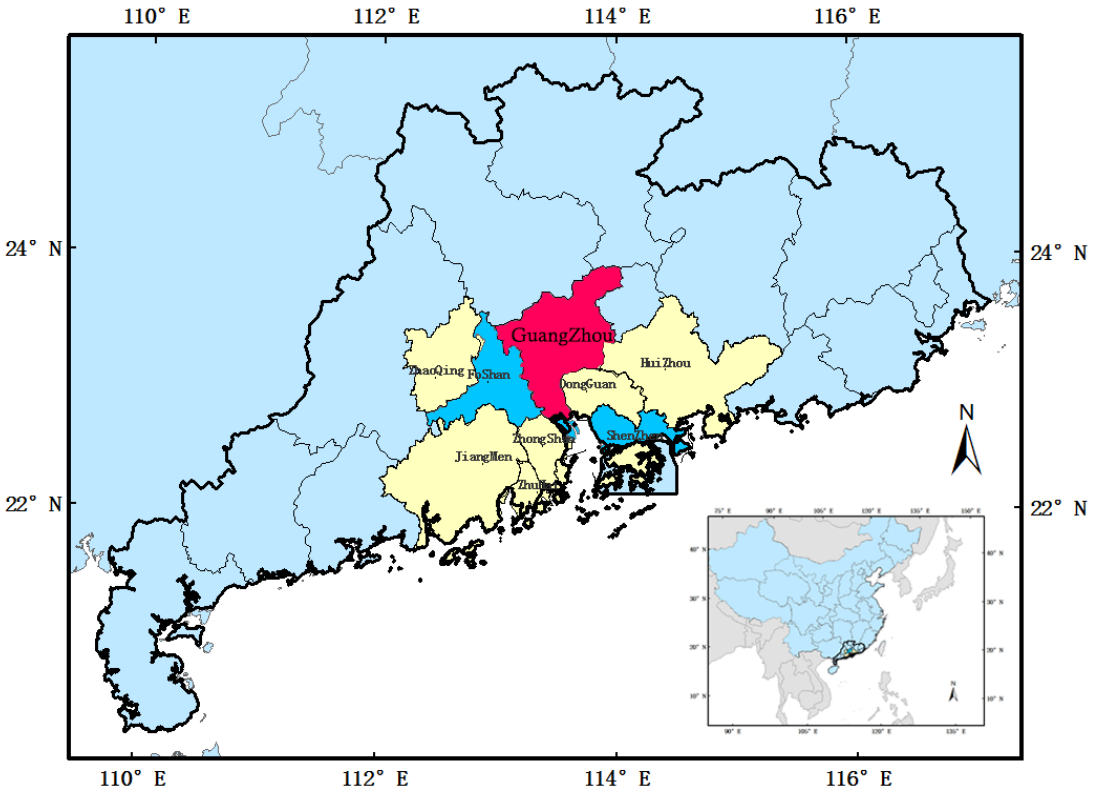

703

704 Fig. 1 Map of Guangdong Province with 9 cities of the inner PRD highlighted

705

706

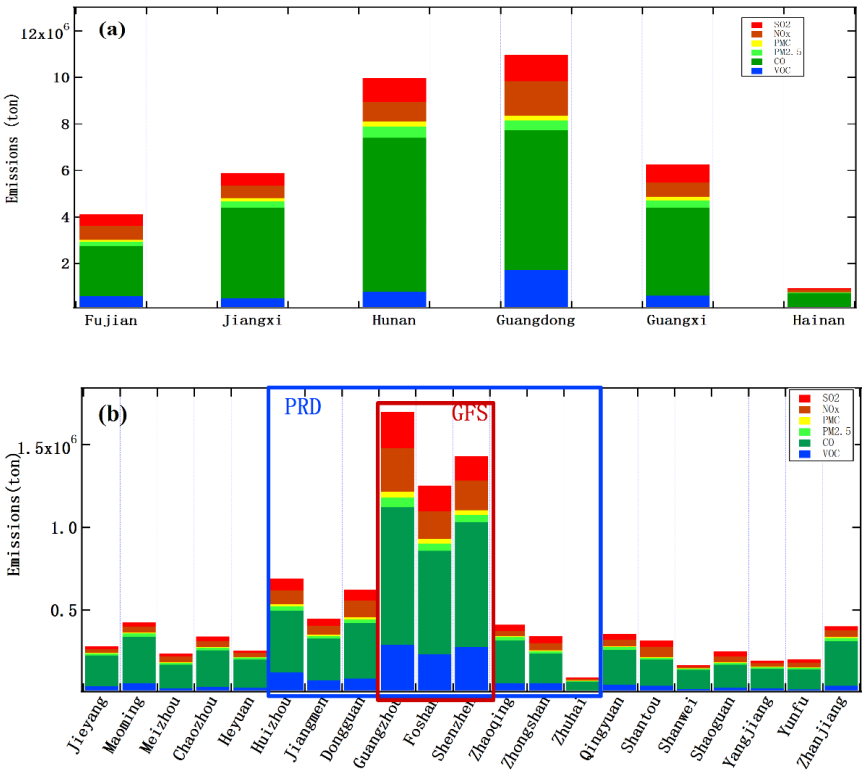

707

708 Fig. 2 Emissions categorized (a) by province in southern China and (b) by city in

709 Guangdong Province (The blue square highlights all cities of inner PRD, and the red

710 square highlights 3 cities of inner PRD, namely, Guangzhou, Foshan and Shenzhen)

711

712 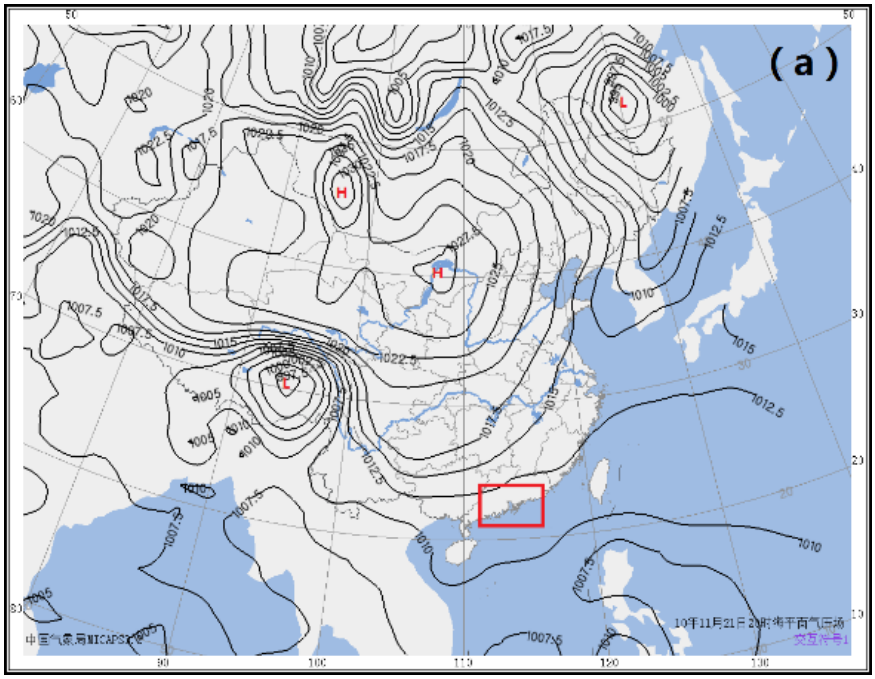

713 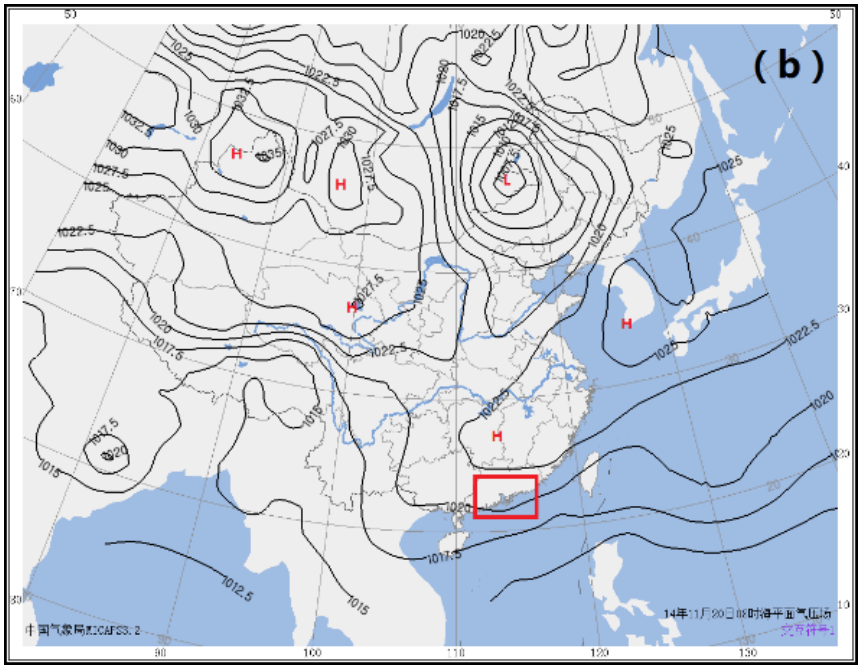

714 Fig. 3 Weather charts of an FC-affected event at 20 LST on Nov 21 2010 (a) and an

715 SP-affected event at 08 LST on Nov 20 2014(b). The red rectangle shows the PRD

716

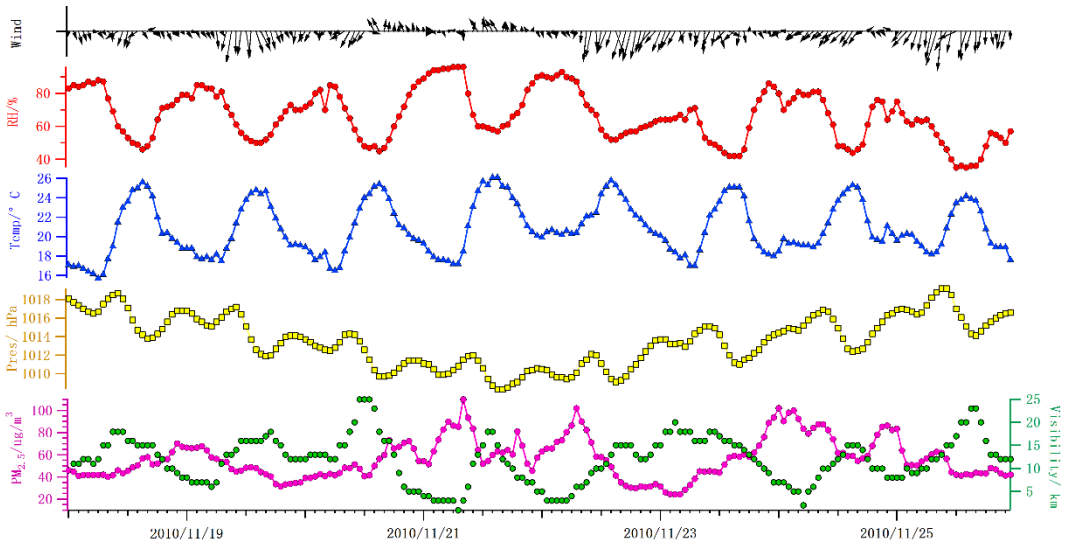

717

718 Fig. 4 Diurnal variation of surface wind, relative humidity, pressure, temperature,

719 $PM_{2.5}$ and visibility under the FC-affected weather system in November 2010.

720

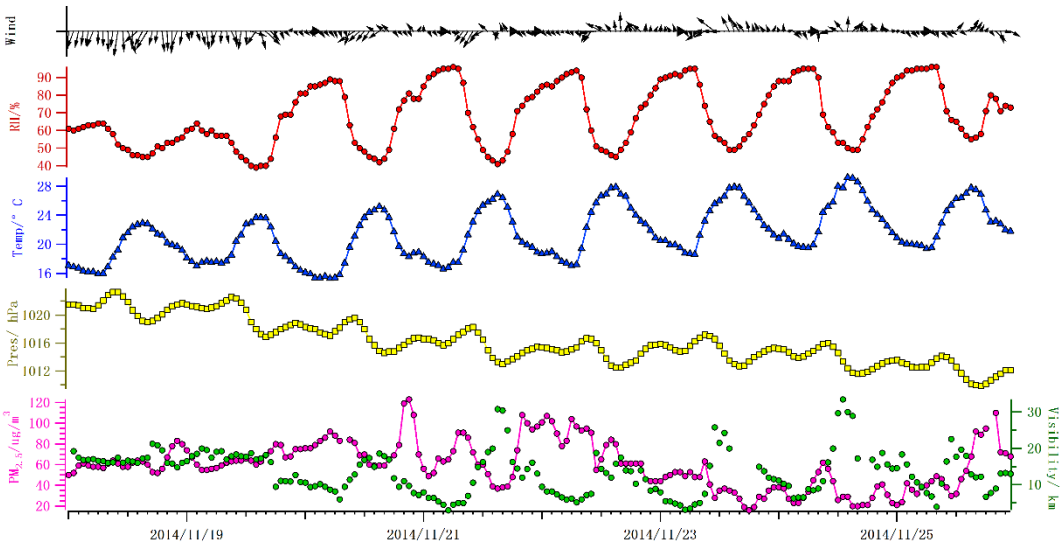

721

722 Fig. 5 Diurnal variation of surface wind, relative humidity, pressure, temperature,

723 $PM_{2.5}$ and visibility under the SP-affected weather system in November 2014.

724

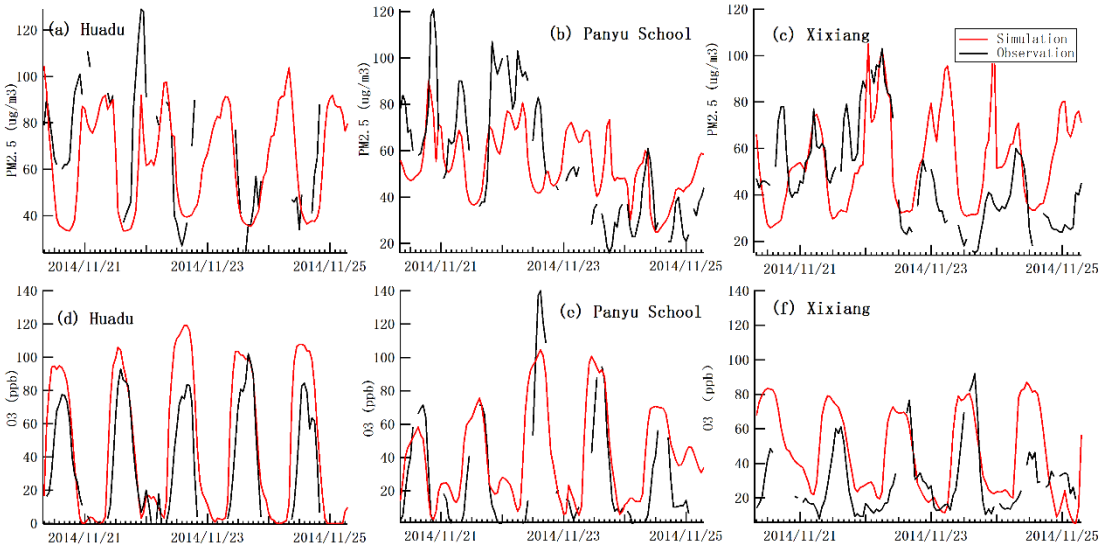

725

726 Fig. 6 Comparisons of simulated and observed $PM_{2.5}$ and O_3 at Huadu (a suburban

727 site in northern Guangzhou), Panyu School (an urban site in southern Guangzhou) and

728 Xixiang (a coastal urban site in Shenzhen) during the SP-affected event.

729

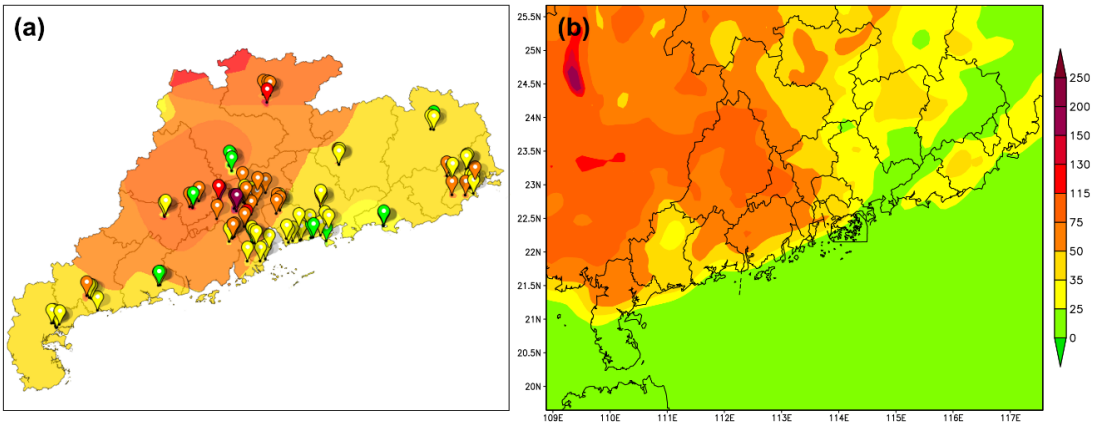

730

731 Fig. 7 Spatial comparison between observed $PM_{2.5}$ and simulated $PM_{2.5}$ over the PRD.

732 (a is the observed $PM_{2.5}$, the pins represent GDEPA monitoring stations, and the

733 contours were interpolated using monitoring values; b is the modelled $PM_{2.5}$)

734

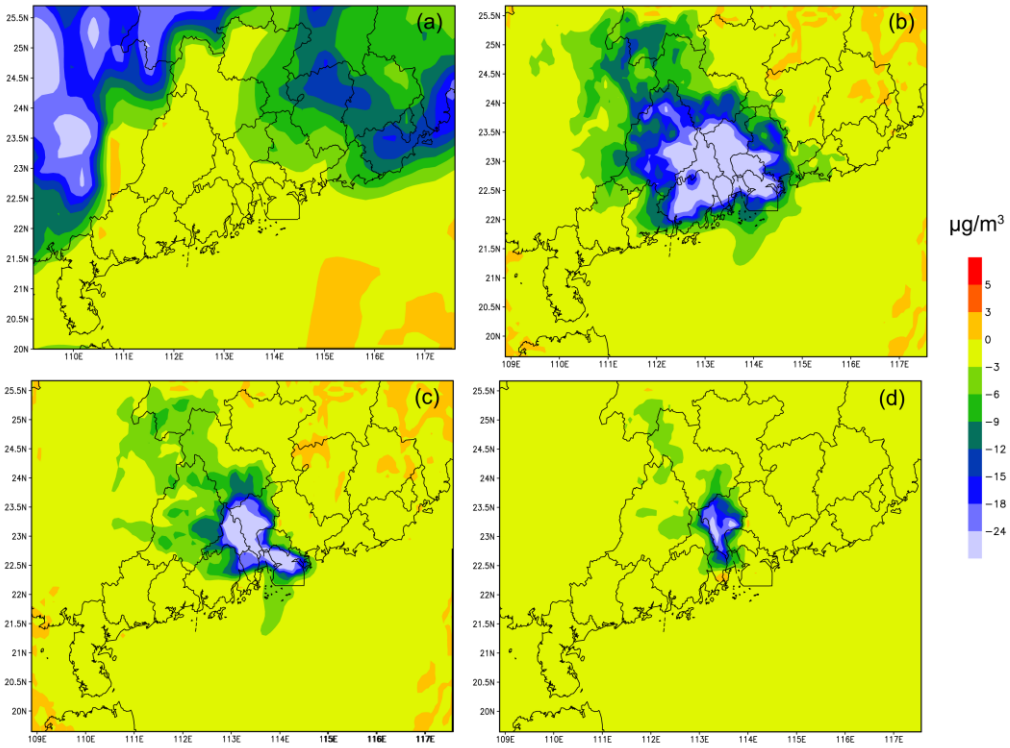

735

736 Fig. 8 Contributions from different source regions to average 08:00 $PM_{2.5}$ during the

737 haze days of the SP-affected event. (a) shows the impact of emissions from outside

738 Guangdong, (b) shows the impact of emissions from the PRD, (c) shows the impact of

739 emissions from the GFS, (d) shows the impact of emissions from Guangzhou

740

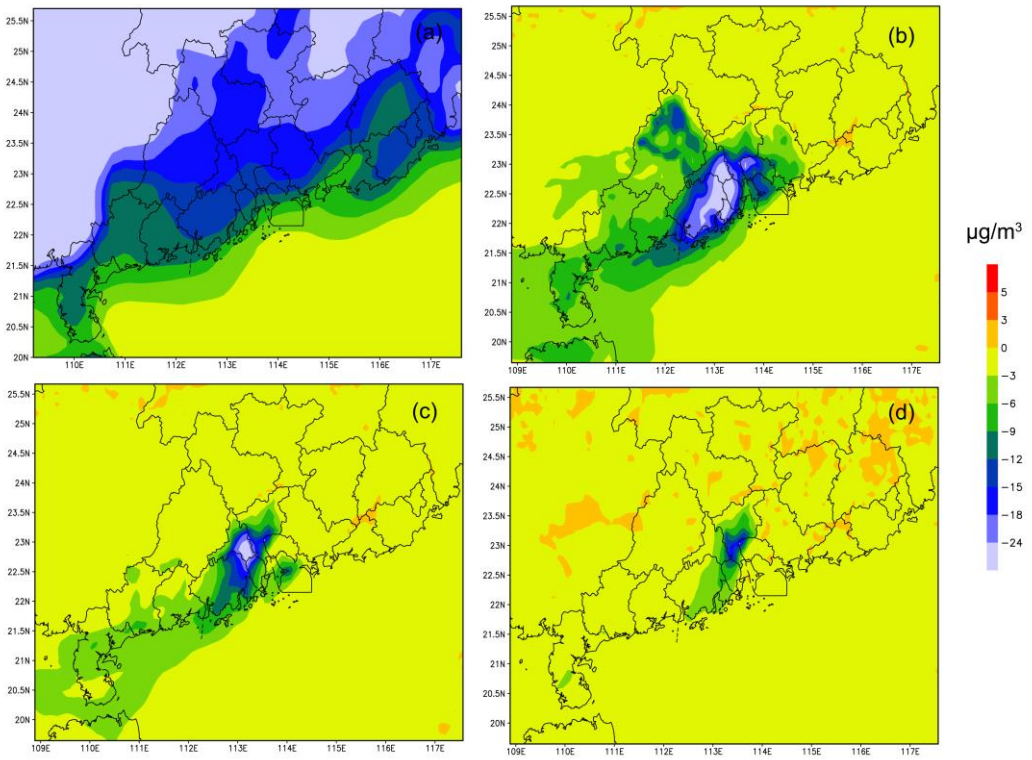

741

742 Fig. 9 Contributions from different source regions to average 08:00 $PM_{2.5}$ during the

743 haze days of the FC-affected event. (a) shows the impact of emissions from outside

744 Guangdong, (b) shows the impact of emissions from the PRD, (c) shows the impact of

745 emissions from the GFS, (d) shows the impact of emissions from Guangzhou.

746

747

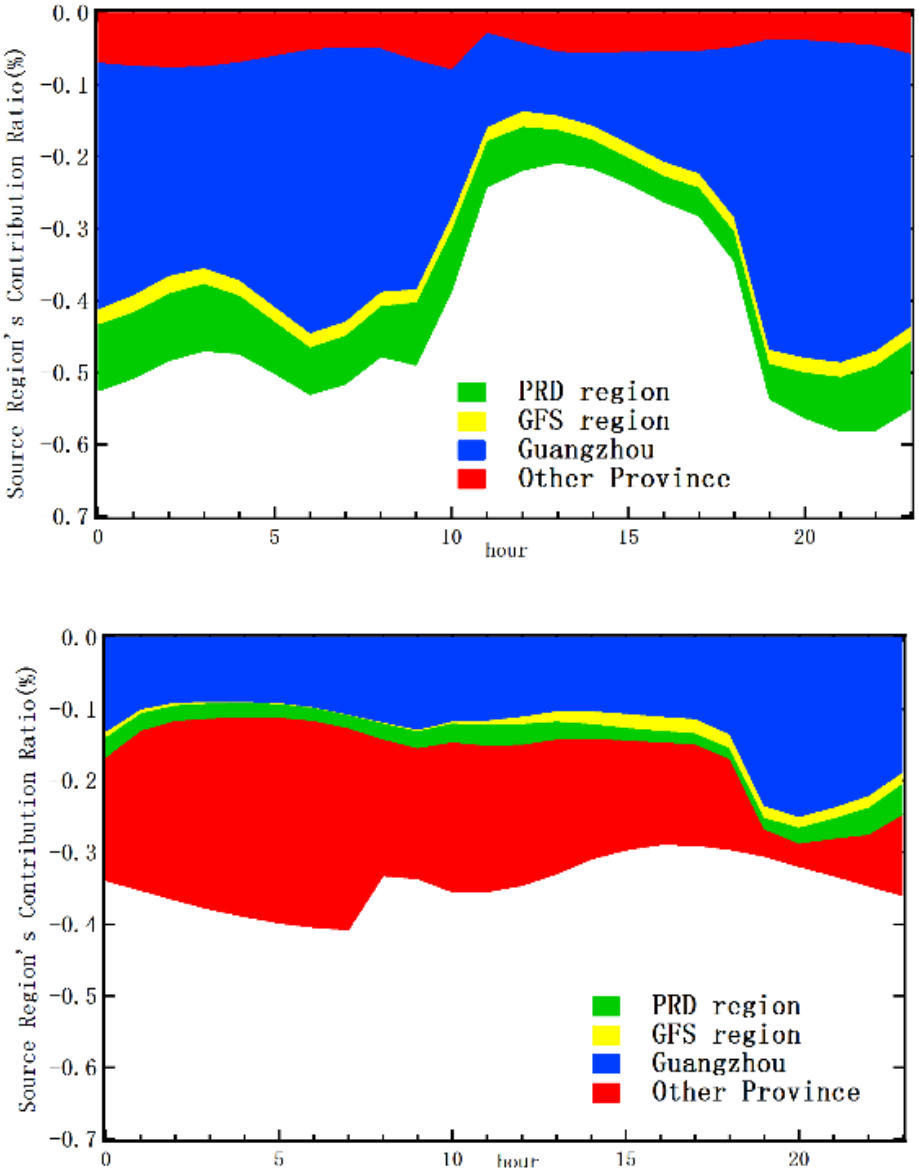

748

749 Fig. 10 $PM_{2.5}$ contributions from different source regions during the SP- and FC-

750 affected events (the top panel shows the SP-affected event; the bottom panel shows

751 the FC-affected event)

752

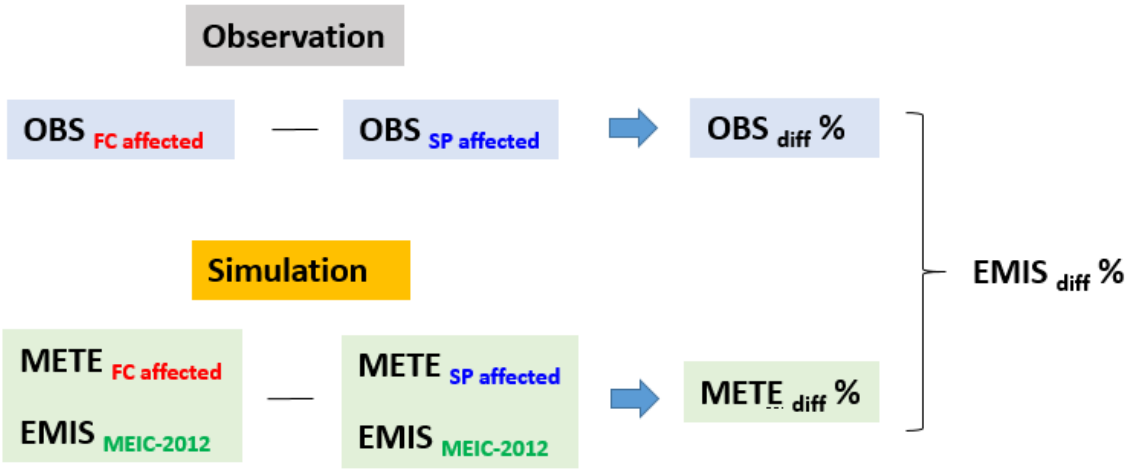

753

754 Fig. 11 A simple method to quantify the impact of meteorology and emissions.

755

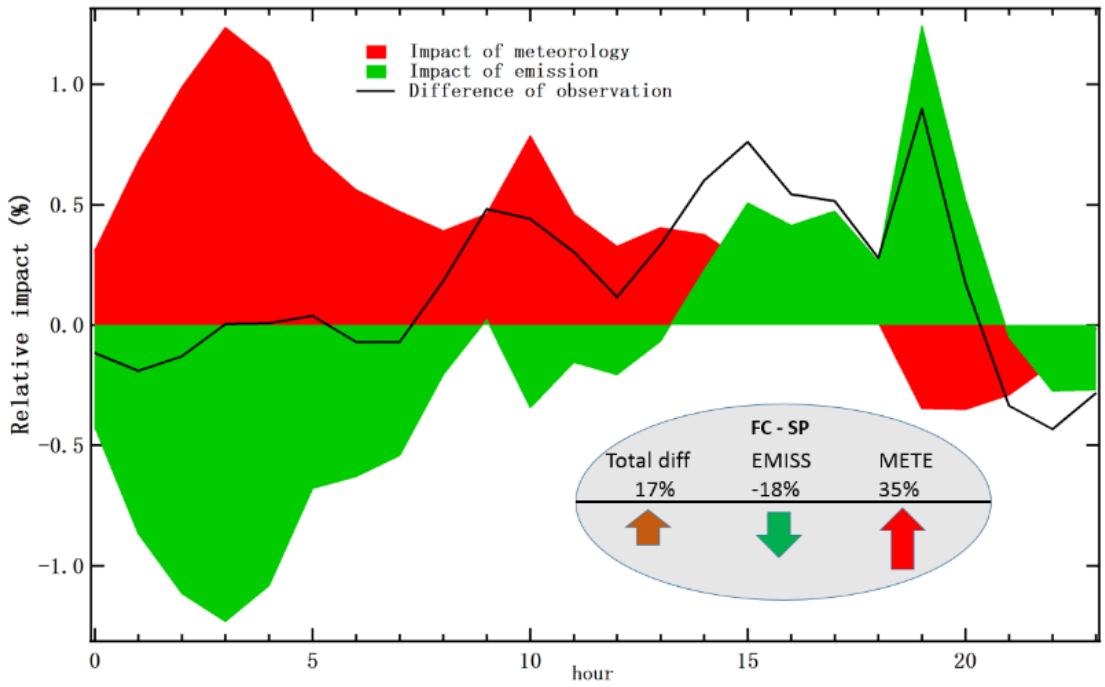

Fig. 12 Relative impact of meteorology and emissions between the FC- and SP-affected events